

Cavendish HEP {97/13

August 1997

Charged Higgs scalar production
in single-top mode (and other)
at future ep colliders
in the Minimal Supersymmetric Standard Model

Stefano Moretti¹ and Kosuke Odagiri¹

Cavendish Laboratory, University of Cambridge,
Madingley Road, Cambridge, CB3 0HE, United Kingdom.

Abstract

We study charged Higgs boson production at future electron-proton colliders in the framework of the Minimal Supersymmetric Standard Model. We focus our attention to the case of single-top production and decay through the channel $t \rightarrow bH^\pm$ and of vector-scalar fusion via $W^\pm \rightarrow H^\pm$ (where $H^\pm = H^\pm; h^\pm$ and A^\pm). We consider the signature $H^\pm \rightarrow \tau^+ \tau^-$ and compare it to the irreducible background from Standard Model interactions. For $M_H < m_t$, the H^\pm signal is accessible through lepton universality breaking if $M_A < 100-120$ GeV at both low and large values of $\tan\beta$. Furthermore, although the bulk of the production cross section comes from single-top events, a sizable contribution due to vector-scalar-scalar interactions should be observable at large $\tan\beta$, this possibly offering some insights into the structure of the scalar sector of the theory. The possibility of the CERN collider running in the LEP-LHC mode is considered in detail.

¹E-mail: moretti, odagiri@hep.phy.cam.ac.uk

1. Introduction and motivation

A charged Higgs boson is a building block of two Higgs Doublet Models (2HDMs), including the Supersymmetry (SUSY) version, as well as of Technicolour (TC) theories [1]. Conversely, such a particle does not belong to the spectrum of the Standard Model (SM). Therefore, its detection would be an unequivocal signal of New Physics.

To date, a lower limit on the value of its mass has been set by the LEP2 data, yielding $M_A > 60 \text{ GeV}$ (for $\tan\beta > 1$) [2], through the (tree-level) relation $M_{H^\pm}^2 = M_W^2 + M_A^2$, so that $M_{H^\pm} > 100 \text{ GeV}$. From arguments related to the request of unitarity of the underlying theory one should expect the upper limit being in the TeV region [3]. Therefore, the mass range allowed for the existence of charged Higgs bosons is indeed vast. Though, if one confines oneself to the case of the Minimal Supersymmetric Standard Model (MSSM) {as we do in the present paper} the decay spectrum of such scalars is rather simple. If one further assumes that the mass scale of the Supersymmetric partners of ordinary matter is above the H^\pm mass, then only two modes dominate the decay phenomenology of the charged Higgs boson. Their reciprocal relevance is dictated by the interplay between the Higgs and top masses. If $M_{H^\pm} < m_t$, then the branching ratio (BR) $\text{BR}(H^\pm \rightarrow \tau^\pm \nu_\tau)$ is the largest (around 98%, for $\tan\beta > 2$) and depends only slightly on the β angle. When $M_{H^\pm} > m_t$, the $H^\pm \rightarrow b\tau$ decay mode is the only accessible channel (with a BR of practically 100% at all $\tan\beta$'s). The mode $H^\pm \rightarrow hW^\pm$ can be relevant only at small values of $\tan\beta$ and in a very narrow mass region right below the $b\tau$ decay threshold [4].

As for the production mechanisms of charged Higgs bosons at colliders, it is likely that one will have to wait for the advent of the future generation of high energy accelerators, in order to detect such particles (see Ref. [1] for a review). In fact, at LEP2, the huge irreducible background in $e^+e^- \rightarrow W^+W^-$ events renders the signal $e^+e^- \rightarrow H^\pm H^\mp$ [5, 6] very hard to extract. In addition, after the recent limit on M_A , the discovery potential of such a machine is rather poor, being confined to a tiny window of a few GeV and only if the CERN e^+e^- machine will reach the energy $\sqrt{s_{ee}} = 205 \text{ GeV}$ [7], which was considered in the context of the 1995 LEP2 Workshop [8].

Since the fact that the charged Higgs mass falls right within the discovery potential of LEP2 is clearly matter of luck, it is far-seeing to look at the case of future machines. At the CERN Large Hadron Collider (LHC), the H^\pm scalar of the MSSM is expected to be copiously produced in top quark decays $t \rightarrow bH^\pm$, provided that $m_t > M_{H^\pm}$ and the value of $\tan\beta$ is low or high enough². Top quarks are produced in $t\bar{t}$ pairs, with a large cross section (we assume $m_t = 175 \text{ GeV}$) [9, 10] and the charged Higgs boson is searched for by means of the leptonic signature $H^\pm \rightarrow \ell^\pm \nu_\ell$. Since neutrinos prevent one from reconstructing the Higgs mass from the momenta of its decay products, the existence of H^\pm signals in the data can be inferred only from an excess of ℓ production with respect to what is predicted in the SM (the lepton universality breaking signal).

In contrast, if $M_{H^\pm} > m_t$ the chances of detection at the LHC are very much reduced. In fact, not only the known production mechanisms of MSSM charged Higgses yield small cross sections, but also the lack of a clean signature contributes to make the signal very poor and overwhelmed by the ordinary QCD background. On the one hand, only the subprocesses $bg \rightarrow tH^\pm$ [11] and $bq \rightarrow bq^0H^\pm$ [12] can be of some help

²The minimum of the $t \rightarrow bH^\pm$ decay rate is at about $\tan\beta = 6$.

if $M_H < 300 - 400 \text{ GeV}$ [1] (and large values of $\tan \beta$ in the second case, too). On the other hand, in order to extract the signal from the huge $W + \text{jets}$ noise typical of hadron-hadron colliders [13], one would really need to reconstruct the Higgs mass resonance through the decay chain $H \rightarrow b\bar{t} \rightarrow b\bar{b}W \rightarrow b\bar{b}jj$ (where j represents a jet from the W decay), procedure which relies on very high b -tagging performances and jet resolution (and dedicated 'tricks' to trigger the 'striplepton' from the primary top in the $t\bar{t}$ production [11])³.

At the Next Linear Collider (NLC) [17][22], H detection looks easy, though the discovery potential of such a machine is far from being decisive [23]. Once again the crucial point is the heavy mass range. Being an e^+e^- collider, it can boast the advantage of a much smaller QCD noise (as compared to hadron-hadron machines), however, in this case is the maximum centre-of-mass (CM) energy which sets the upper limit on the detectable H mass. For a $\sqrt{s_{ee}} = 500 \text{ GeV}$ NLC [17, 18], one clearly cannot go beyond the value $M_H \approx 220 \text{ GeV}$, as the main production channel is $e^+e^- \rightarrow H^+H^-$ [6]. Furthermore, the e^+e^- running modes (using Compton back-scattered laser photons [24, 25]) at the NLC do not improve the prospects of MSSM charged Higgs detection [26], as the three viable channels $e^+e^- \rightarrow e^+H^+H^-$, $e^+e^- \rightarrow e^-H^-A$ [27] and $e^+e^- \rightarrow H^+H^-$ [28] only allow one to cover adequately the intermediate Higgs mass range. In this context, much higher CM energies [22] would be more helpful, though the realisation of such designs is well into the next millennium.

Since the detection of heavy charged Higgs scalars of the MSSM is far from certain even after the end of the LHC and NLC era, it is particularly worthwhile to assess already at present the discovery potential of these particles of other planned machines too. This will anyway be beneficial, whichever the outcome of the actual analyses is. In fact, these will either establish the impracticability of charged Higgs boson searches or, more interestingly, provide a new experimental ground where to test the MSSM theory. In particular, they could well extend the present coverage in mass and/or offer alternative production mechanisms of charged Higgs scalars, the latter involving new interactions other than the $t \rightarrow bH$ decay (LHC) and the QED-like vertex $e^+e^- \rightarrow H^+H^-$ (NLC).

We turn our attention to the case of future electron (positron)-proton colliders, running with a CM energy in the TeV range⁴. The physics of ep colliders, in conjunction with the discussed possibility of their running in the p mode [33], has been recently under renewed and active discussion [34]. A possible design was proposed and several experimental simulations performed already in 1990 (during the Aachen LHC Workshop [35]), for a LEP-LHC [36] machine obtainable crossing one electron (positron) beam from LEP and a proton one from the LHC [37]. For a 100 GeV electron (positron) and a 7 TeV proton, the total energy in the frame of the colliding particles would be $\sqrt{s_{ep}} = 1.7 \text{ TeV}$. Depending on the relative values of the electron (positron) and proton

³Note that if SUSY decays of charged Higgs bosons are allowed, several novel signatures (mainly involving charginos and neutralinos [14, 15, 16]) could be exploited [1], though their phenomenology is at present very much SUSY-parameter dependent for being of experimental concern. This issue is however beyond the scope of this paper.

⁴The Higgs discovery potential of the only ep collider operative at present, i.e., HERA at DESY, has been shown to be very poor [29]. As for charged Higgses in the MSSM, the available production channels are via gg [30], g [31] and q fusion [32], all being significant only for very light scalar masses (strongly disfavoured by the experiment).

energy, the instantaneous luminosity should vary in the range $(5 \cdot 10^{31} - 4 \cdot 10^{32}) \text{ cm}^{-2} \text{ s}^{-1}$ [38]. We convert these values into 1 fb^{-1} of integrated luminosity per annum, number that we will adopt as a default in the forthcoming discussions. The attractiveness of such a machine is that it allows for a cleaner environment thanks to the suppression of the initial state QCD noise while maintaining the collision energy at the TeV scale.

To our knowledge, no detailed study of MSSM charged Higgs boson production at future ep colliders exists in the literature, apart from a preliminary analysis carried out in Ref. [39]. However, we do expect that charged Higgs bosons of the MSSM can be abundantly produced in electron (positron)-proton collisions at the TeV scale. In particular, it is the purpose of this paper to study the reaction (e.g., for the case of a positron beam)

$$e^+ b \rightarrow e b H^+; \quad (1)$$

proceeding through the two subprocesses

$$e^+ b \rightarrow e t \rightarrow e b H^+ \quad (2)$$

(i.e., single top production and decay)⁵ and

$$e^+ b \rightarrow e b W \rightarrow e b H^+ \quad (3)$$

(i.e., vector-scalar fusion). If one considers two-body fermion decays of the charged Higgs, then the graphs contributing to

$$e^+ b \rightarrow e b H^+ \rightarrow e b f f^0; \quad (4)$$

(where $f f^0$ represents, e.g., $\tau^+ \tau^-$ or $b \bar{b}$) are those depicted in Fig. 1.

We are motivated to study this process following the results presented in Ref. [12], where the hadronic counterpart of process (4) was considered (i.e., $e^+ \rightarrow q$ and $e \rightarrow q^0$, with $q^{(0)}$ light quark). There, it was shown that bq fusion could effectively help in increasing the chances of H^\pm detection at the LHC, also above the $H^\pm \rightarrow b \tau$ decay threshold. This is due to three main reasons: (i) a large content of b -quarks inside the proton at the LHC; (ii) the strength of the Yukawa couplings of the neutral Higgs bosons of the MSSM to the b -quarks increasing with the value of $\tan \beta$ (graph 2); (iii) vertex tagging performances of the LHC detectors which are expected to be ideal.

One should expect this channel to be similarly effective also at a future ep collider, as the large content of b quark inside the scattered hadron is guaranteed by the TeV energy of the LHC beam and the capabilities of the LHC vertex detector should be maintained while running the CERN machine in the ep mode. Along with the signal (1) we will also study several SM-like ‘irreducible’ backgrounds, on the same footing as in Ref. [12]⁶.

The plan of the paper is as follows. In the next Section we discuss some details of the calculation. Section 3 presents our results whereas in the last one we outline some brief conclusions and possible prospects.

⁵Here and in the following h refers collectively to the three neutral Higgs scalars of the MSSM: H , h and A .

⁶For the time being, we neglect considering H^\pm signals via top production and decay in double mode, through $g \rightarrow t \bar{t}$, as the corresponding cross section is, at the TeV scale and for $m_t = 175 \text{ GeV}$, a factor of 100 smaller than that of single-top [40, 41].

2. Parameters

As for the details of the computation techniques of the relevant Feynman amplitudes⁷, for the choice of structure functions as well as for the numerical values of the SM parameters used in this paper, we refer the reader to Ref. [41]⁸. The only exception is the top width, which has been modified in order to allow for SUSY decays of the top quark. Concerning the MSSM parameters, we assume a universal soft Supersymmetry-breaking mass [42, 43] $m_{\tilde{u}}^2 = m_{\tilde{d}}^2 = m_{\tilde{q}}^2$ and negligible mixing in the stop and sbottom mass matrices, $A_t = A_b = 0$. Under these conditions, the one-loop corrections to the masses of the MSSM neutral CP-even Higgs bosons and to the mixing angle are introduced via simple relations (see Refs. [44, 42]), which we have already recalled in Ref. [12]. For the MSSM charged Higgs mass we have maintained the tree-level relation mentioned in the Introduction, since one-loop corrections are small compared to those for the neutral Higgses [43]. As it is impractical to cover all possible regions of the MSSM parameter space $(M_A; \tan \beta)$, we have decided to concentrate here on the two representative values $\tan \beta = 1.5$ and 30. and on masses of the pseudoscalar Higgs boson A in the range $60 \text{ GeV} < M_A < 220 \text{ GeV}$.

As was done in Ref. [41], we consider (as an illustration, see the discussion there) the case of positron beams from LEP (i.e., of e^+b -fusion). The total CM energy $\sqrt{s_{\text{ep}}}$ of the colliding particles will span in the range between 300 GeV (i.e., around the HERA value) and 2 TeV. However, we will focus our attention mainly to the case of a possible LEP2–LHC accelerator, as illustrated in the previous Section.

Before proceeding with the discussion of the results, we present in Tab. I the cross sections of the signal process (1) evaluated at the LEP2–LHC energy for twenty-four different sets of structure functions. This is done in order to estimate the theoretical error due to the b Parton Distribution Function (PDF) (see discussion in Ref. [41]). By using the very last generations of structure functions to be found in the literature, we estimated the PDF dependence to be approximately 25%, with the maximum value of the total cross section differing from the minimum one by 180 fb. We believe such uncertainty to be already at the present time a quite small error, so to motivate further and more detailed simulations (including hadronisation, detector effects, reducible background [40, 45]) of charged Higgs phenomenology at future ep colliders.

3. Results

We present the total cross section rates for process (1) in Figs. 2{3⁹. Generally the cross section at $\tan \beta = 30$: (Fig. 2a) is greater than that at $\tan \beta = 1.5$ (Fig. 2b). This

⁷Note that the analytical expression for the amplitude of the signal process (4) is identical to that given in the Appendix of Ref. [12] for the hadronic cases, provided one replaces there p_U and p_D (i.e., the light quark four-momenta) with p_e and $p_{\bar{\nu}}$ (i.e., the electron/neutrino ones).

⁸Note that, while in Ref. [41] several different choices of the renormalisation/factorisation scale were adopted, in the present analysis we stick to the unique ‘running value’ $\mu' = \sqrt{s}$, that is the CM energy at parton level.

⁹Incidentally, we mention that, as a check of our results, we have verified that the rates presented here for the single-top subprocess in Narrow Width Approximation (NWA) reproduce quite well the cross section for on-shell top production

$$e^+b \rightarrow e^+t; \quad (5)$$

is because the contribution to the total cross section of subprocess (3) is negligible at $\tan \beta = 1.5$ (Fig. 3a) whereas it is sizable at $\tan \beta = 30$: (Fig. 3b) and also because the top BR into $b\bar{H}$ pairs is higher at larger $\tan \beta$'s (see Fig. 4). These features can be interpreted in terms of scalar-fermion vertices.

In the case of diagram 1 in Fig. 1 the enhancement due to the $m_b \tan \beta$ scalar coupling to the b is greater than the suppression due to the reduced strength $1/\tan \beta$ of that to the top quark. In case of diagram 2 in Fig. 1, one should recall that, with increasing $\tan \beta$, the $A b \bar{b}$ vertex grows (rather quickly, as $\tan \beta$) and so do the $H b \bar{b}$ and $h b \bar{b}$ ones, though less sharply (they are proportional to $c = c$ and $s = c$, respectively). As for the $W H$ vertex, things go the opposite (same) way for the heavy (light) Higgs scalar H (h): that is, the vector-(neutral) scalar-(charged) scalar coupling tends to decrease (increase) with increasing $\tan \beta$, though only for values of $M_A < 140$ GeV. For heavier M_A 's the role of the two scalars is interchanged. Finally, the $W A H$ interaction shows no dependence on the MSSM parameters.

Fig. 3 emphasises the point that, at LEP-LHC energies and for a yearly luminosity of 1 fb^{-1} , a charged Higgs particle of less than the top mass (corresponding to $M_A = 140$ GeV) can be largely produced. For $M_A > 140$ GeV, the rate begins to be very small with a strong decrease of the cross sections for an increasing Higgs mass, this being mostly due to the fact that the dominant single-top diagram gets small because of the suppressed BR of top quarks into $b\bar{H}$ pairs. Where the vector-scalar fusion diagram plays a dominant role (i.e., for $M_A > 150$ GeV), are phase space effects that are more relevant as compared to those due to the couplings (the latter have a complicated dependence on M_A for different vertices and scalar bosons as well), since the overall feature is a decrease of the cross section at larger M_A 's.

The dependence of the production rates on the CM energy $\sqrt{s_{\text{ep}}}$ is governed by the kinematic suppression on the single-top production and at low energies, say $\sqrt{s_{\text{ep}}} < 500$ GeV, the cross section falls to negligible scales for all combinations in the plane $(M_A; \tan \beta)$. In general, although the rate of process (1) is small at existing collider energies ($\sqrt{s_{\text{ep}}} = 300$ GeV at DESY leads to a total cross section of less than 0.1 fb , which is negligible given the current integrated luminosity of about 20 pb^{-1} [46] at each of the two experiments), it increases markedly near the TeV scale. At the LEP2-LHC energy it is easily observable already after one year of running as long as single-top production dominates. As a matter of fact, when this is no longer the case (i.e., when $M_H > m_t$, the 'critical' heavy range), production rates fall below detection level. In fact, the cross sections never exceed the 1 fb value. This makes immediately the point that the discovery potential of future ep colliders is realistically confined to the intermediate M_H range only, where the coverage furnished by the LHC and the NLC will probably be more than adequate.

However, the production mechanism is here different, as it also proceeds (other than via top decays) through additional diagrams involving the neutral Higgses whose effects are perceptible over a sizable portion of the MSSM parameter space, provided $\tan \beta$ is large enough (see Fig. 2d). This is particularly true at small values of $\sqrt{s_{\text{ep}}}$ (where the kinematic threshold suppression on $t \rightarrow b\bar{H}$ is active, i.e., $\sqrt{s} \approx m_t$) and M_A as well.

and are compatible with those presented in Ref. [41] for the SM decays $t \rightarrow bW$ once the MSSM top width is consistently adopted.

At those energies though, the total cross section of process (1) is too low. In contrast, this is no longer the case at LEP2–LHC energies, where the effects of graph 2 are still significant (for large $\tan \beta$'s) and act on a comfortably large total cross section. On its own, subprocess (3) yields (at $\sqrt{s_{\text{ep}}} = 1.7 \text{ TeV}$) a rate of approximately 2 fb (for $M_A = 140 \text{ GeV}$ and $\tan \beta = 30$). However, a somewhat stronger effect appears through the (negative) interference between the two graphs in Fig. 1, reducing the single-top rates by 10% or so. This is presumably the effect that one should search for, even because it will probably not be possible to separate efficiently the two components (2) + (3) of the cross section, as the charged Higgses produced would decay leptonically with the neutrinos escaping the detectors. Therefore, the $t \rightarrow bH^\pm$ resonance cannot be reconstructed and exploited to remove single-top events from the complete sample. For 1 fb⁻¹ of yearly luminosity, the above rates mean that some 5 events out of the 59 expected from single-top production should be missing¹⁰. Furthermore, one should recall that these 'production' rates can be fully exploited also at 'decay' level as the channel has a BR of practically one at large $\tan \beta$'s. Such effect could well be used to test possible anomalous couplings in the Higgs sector of the MSSM and/or in constraining possible gauge violations affecting the $W-H$ vertex.

In the remainder of the paper, since the only H^\pm mass range that can be explored at future TeV ep colliders is below the value of m_t , we will consider decays of the charged Higgs boson only: that is, the two-to-four body reaction

$$e^+ b \rightarrow e^- b H^+ \rightarrow e^- b \nu_\tau^+ : \quad (6)$$

The signature that one should expect from this process would then be a ν -jet (which we assume easily distinguishable from those originated by quarks and gluons), a b -jet (which we assume to be vertex tagged with efficiency close to unity) and appreciable missing momentum, and the signal should be revealed as a clear excess with respect to the rates due to SM processes (the recalled lepton universality breaking signal).

Fig. 5 plots the differential distributions in various kinematic quantities which can be reconstructed from the detectable particles in the final state of process (6). The distribution in transverse momentum p_T shows that neither cuts in p_T nor cuts in p_T^{miss} will affect the total cross section dramatically, whereas that of R , the azimuthal-pseudorapidity separation defined by $R = \sqrt{(\Delta\phi)^2 + (\Delta\eta)^2}$ (where $\Delta\phi$ is the azimuthal angle and $\Delta\eta$ the pseudorapidity) indicates that the requirement of an isolated lepton may strongly affect the event rate. The majority of events are found within $R < 1.5$, which is about 90 degrees in the azimuthal angle. This is because the bottom quark jet and the tau come from the energetic top quark. Thus, at lower energies the azimuthal-pseudorapidity spread in the top quark decay products will be larger and hence the requirement of an isolated lepton not so severe. The distribution of the missing transverse momentum is small at low missing p_T and indicates that the charged current cut in missing transverse momentum will not affect the event rate significantly.

Tab. II shows the total cross section after the acceptance cuts. The following constraints were implemented (see [40] for discussions): $p_T^+; p_T^b > 20 \text{ GeV}$, $p_T^{\text{miss}} > 10 \text{ GeV}$

¹⁰Note that, if the electron (positron) beam will have a 50 GeV energy, this yielding $\sqrt{s_{\text{ep}}} = 1.2 \text{ TeV}$, so to increase the luminosity (see Ref. [36]) by a factor of ten, one would then rely on a statistically more significant sample, as at that energy the depletion due to interference effects is around 8% (see Figs. 2d). However, we do not consider here such a possibility.

and $R_{\text{tag}} > 0.7$. We have not implemented any cuts on the pseudorapidity, as the events are all concentrated in the detectable j - j region: see the spectra in the two lower frames of Fig. 6.

In Fig. 6 we also plot the distributions in the invariant mass of the only visible pair of particle momenta, the b and \bar{b} -ones, i.e., M_b . This is done in order to possibly aid further the signal selection, as this cannot rely on the kinematic reconstruction of the charged Higgs boson mass, because of the $\bar{\nu}_\tau$ -neutrino. In particular we would like to point out that there is a kinematic interplay between, on the one hand, the top, tau and bottom masses and, on the other hand, that of the boson produced in the top decay, inducing a cut-off on the maximum value of M_b . This should clearly be different for the ordinary SM-like backgrounds, particularly that due to single-top production followed by $t \rightarrow bW$ (the dominant one, see Ref. [41]). In general, assuming that both the top quark and the decay boson are on-shell, the cut-off is given by $M_b^{\text{max}} = \sqrt{m_t^2 + m_b^2 + M_V^2} - M_V$, with $M_V = M_H$ or M_W . For example, at low M_A , the cut-off in the roughly triangular distributions in M_b is close to the top mass as expected, whereas at high M_A , as the charged Higgs mass tends to the top mass, the cut-off is smaller since the momenta carried by the bottom quark become less energetic. For comparison, in Fig. 7 we present the same M_b distribution for the background processes

$$e^+b \rightarrow \bar{\nu}_\tau b^+; \quad (7)$$

and

$$e^+b \rightarrow \bar{\nu}_\tau b^+; \quad (8)$$

both proceeding via a $W^{+(*)} \rightarrow \bar{\nu}_\tau$ splitting (see Figs. 1c and d of Ref. [41], respectively). To facilitate the comparison between the two figures, the normalisation has been set to unity. We see that the spectrum of the MSSM signal is significantly harder (softer) than the SM-like one from process (7) for smaller (larger) values of M_A , at all $\tan\beta$. There is a sort of degeneracy between the two processes (6) and (7) for $M_A = 100$ GeV, rather than for smaller M_A 's (thus for M_H 's closer to M_W). This is due to the additional diagrams entering in the latter reaction, which do not suffer from the kinematic cut-off. Also note that for the background there is no dependence of the shape on the actual values of the MSSM parameters. As for events of the type (8), the distribution is rather flat, with no evident kinematic peak. Thus, apart for $M_A = 100$ GeV, the M_b spectrum should indeed help in disentangling the H signals from the irreducible background.

The total cross sections of process (7) are presented in Tab. III, for the same choice of the $(M_A; \tan\beta)$ parameters as in the previous one. We do not reproduce here the rates for process (8) as these are two orders of magnitude smaller, around 4.8 fb, and with no dependence on M_A and/or $\tan\beta$, confirming that the background that does not involve the on-shell top production will not affect the detection of H signals at all, even in case of poor performances in measuring the jet charge of the b -jet. The dependence of the background (7) on the MSSM parameters can be traced back to the simple fact that the greater the BR for the top decay into H the smaller the one for the background process $t \rightarrow bW^+$. The dependence entering in the total cross section of process (7) through the neutral Higgs mediated diagrams (see Fig. 1c of Ref. [41]) is indeed negligible.

It can be seen that for $\tan \beta = 1.5$ the lepton universality breaking signal is significant over the background for M_A up to about 100 GeV, whereas at $\tan \beta = 30$: the signal is significant up to 120 GeV. Therefore, a combination of event rate counting and M_b distribution studies should allow for the detection of charged Higgs bosons of the MSSM over a large portion of the $(M_A; \tan \beta)$ plane.

4. Summary and conclusions

The phenomenology of charged MSSM Higgs bosons H^\pm produced from initial state bottom sea quarks at future ep colliders was studied, mainly focusing our attention to the case of the planned LEP2-LHC accelerator with the positron (electron) beam energy of 100 GeV and the proton one of 7 TeV. The design of such collider was already proposed in 1990 as a possible extension of the LEP and LHC programmes at CERN and the physics of such machines has been the object of a recent renewed interest. The motivation for our analysis was twofold. First, it is quite clear that neither the LHC nor the NLC will probably be able to cover adequately the heavy mass range of the H^\pm scalar (when $M_{H^\pm} > m_t$). Second, in the accessible intermediate mass range (i.e., $M_{H^\pm} < m_t$), charged Higgs bosons are produced in either top decays (LHC) or via $! H^+ H^-$ splitting (NLC), so that the insight on the phenomenology of the Higgs sector of the MSSM is only connected to a test of the β -dependence entering in the $H^\pm b t$ vertex, as the $H^+ H^-$ one only depends on the electromagnetic coupling constant. In our opinion, it was therefore important to assess the potential of future ep colliders in the above respects.

Assuming 1 fb^{-1} of integrated luminosity per year of running, the detectable rate was found to vary in the range 2-300 events per annum, depending on the Higgs masses and $\tan \beta$. The uncertainty due to the structure functions was found to be rather small already at the present time, around 25%, and is expected to diminish significantly before new ep machines will enter operation. The main prity of the Higgs boson production, in the range of collider energies relevant to our study (i.e., between 300 and 2000 GeV), occurs for values of M_{H^\pm} below the top mass, where the dominant decay mode of charged Higgs bosons is into $\tau^+ \tau^-$ pairs. For such values of M_{H^\pm} the event rate is primarily due to single-top quark production and decay in the charged current process $e^+ b \rightarrow e^- t \rightarrow e^- b H^+$.

Although the production of H^\pm scalars via a top decay is also the signature typical at the LHC, the additional feature of MSSM charged Higgs boson production at future ep colliders is a sizable contribution from vector-scalar fusion diagrams of the type $e^+ b \rightarrow e^- W^\pm \rightarrow e^- b H^\pm$ involving the neutral Higgs bosons of the MSSM (i.e., H^0, h, A) in virtual state, provided $\tan \beta$ is large. This is particularly true for small M_A 's and for values of the CM energy of the ep collisions below 500 GeV (when the 'partonic' CM energy is often below the single-top production threshold), where corrections to the cross section can amount to up to +20% of the single-top rate. However, at typical LEP2-LHC energies the effect is still significant and should be visible through a negative interference between single-top and vector-scalar fusion diagrams, which depletes the single-top event rate by up to 10% or so, for $140 \text{ GeV} < M_A < 160 \text{ GeV}$. Such effect clearly represents a test of the Higgs sector of the MSSM as well as

a constraint on possible gauge violation effects which could manifest themselves in the $W-H$ vertex. For values of M_H in the heavy range, the single-top production rates fall at negligible levels and the kinematic suppression on the vector-fusion mechanism is such that the production cross section is below detection level, even for optimistic luminosities. Therefore, as for heavy charged Higgses of the MSSM, no further H detection potential other than that already provided by the LHC and NLC should be expected by future ep colliders at the TeV scale.

Finally, several kinematical quantities associated with the momenta which can be reconstructed from the visible particles of the signature b^+E_{miss} were studied. In general, LHC-type detectors should provide an adequate coverage (in pseudorapidity and transverse momentum) of the phase space available to events of the type $e^+b \rightarrow e^+bH^+ \rightarrow e^+b^+H^+$. In addition, the invariant mass of the b^+ -pair can be profitably exploited in separating the H signal events from the irreducible SM-like electroweak background, which we have evaluated consistently. Indeed, the lepton universality breaking signature can be used as a mean to recognise MSSM charged Higgs events for masses up to 100{120 GeV (that is $M_H = 130-145$ GeV) for both small and, more markedly, large values of $\tan\beta$.

We believe that charged Higgs boson phenomenology in the context of MSSM can be a relevant experimental issue at future ep colliders, and we look forward to additional studies of (possibly) new production mechanisms as well as more detailed simulations, including detector and hadronisation effects. To this end, the FORTRAN programs used for this analysis can be obtained from the authors upon request.

5. Acknowledgements

We thank Lorenzo Diaz-Cruz for useful discussions. SM is grateful to the UK PPARC and KO to Trinity College and the Committee of Vice-Chancellors and Principals of the Universities of the United Kingdom for financial support. SM also thank the Theoretical Physics Department in Lund (Sweden), where part of this work was carried out under a grant of the Italian Institute of Culture 'C.M. Lerici' (Ref. #: Prot. I/B1 690).

References

- [1] J.F. Gunion, H.E. Haber, G.L. Kane and S. Dawson, "The Higgs Hunter's Guide" (Addison-Wesley, Reading MA, 1990).
- [2] See, e.g.:
The Aleph Collaboration, preprint CERN-PPE/97-071, June 1997.
- [3] P. Langacker and H.A. Weldon, Phys. Rev. Lett. 52 (1984) 1377;
H.A. Weldon, Phys. Rev. D 30 (1984) 1547; Phys. Lett. B 146 (1984) 59.
- [4] S. Moretti and W.J. Stirling, Phys. Lett. B 347 (1995) 291; Erratum, ibidem B 366 (1996) 451.

- [5] A. Djouadi, J. Kalinowski and P.M. Zerwas, Z. Phys. C 57 (1993) 569.
- [6] S. Komamiya, Phys. Rev. D 38 (1988) 2158.
- [7] S. Moretti and K. Odagiri, J. Phys. G 23 (1997) 537.
- [8] Proceedings of the Workshop 'Physics at LEP 2', eds. G. Altarelli, T. Sjöstrand and F. Zwirner, CERN Report 96-01.
- [9] ATLAS Technical Proposal, CERN/LHC/94-43 LHCC/P2, December 1994.
- [10] CMS Technical Proposal, CERN/LHC/94-43 LHCC/P1, December 1994.
- [11] J.F. Gunion, H.E. Haber, F.E. Paige, W.-K. Tung and S.S.D. Willenbrock, Nucl. Phys. B 294 (1987) 621.
- [12] S. Moretti and K. Odagiri, Phys. Rev. D 55 (1997) 5627.
- [13] J.F. Gunion, H.E. Haber, S. Komamiya, H. Yamamoto and A. Barbaro-Galtieri, in 'Proceedings of the 1987 Berkeley Workshop on Experiments, Detectors and Experimental Areas for the Supercollider', eds. R. Donaldson and M. G. Ilchiesse (World Scientific, Singapore, 1988).
- [14] J.F. Gunion and H.E. Haber, Nucl. Phys. B 272 (1986) 1.
- [15] J.F. Gunion and H.E. Haber, Nucl. Phys. B 278 (1986) 449.
- [16] J.F. Gunion and H.E. Haber, Nucl. Phys. B 307 (1988) 445.
- [17] Proceedings of the Workshop 'e⁺e⁻ Collisions at 500 GeV. The Physics Potential', Munich, Annecy, Hamburg, ed. P.M. Zerwas, DESY 92-123 A/B/C, 1992-1993.
- [18] Proceedings of the Workshop 'Physics with e⁺e⁻ Colliders', Annecy, Gran Sasso, Hamburg, ed. P.M. Zerwas, DESY 97-100, May 1997.
- [19] Proceedings of the Workshop 'Physics and Experiments with Linear Colliders', Sariselka, Finland, 9-14 September 1991, eds. R. Öröva, P. Eerola and M. Nordberg (World Scientific Publishing, Singapore, 1992).
- [20] Proceedings of the Workshop 'Physics and Experiments with Linear e⁺e⁻ colliders', eds. F.A. Harris, S.L. Olsen, S. Pakvasa and X. Tata (World Scientific Publishing, Singapore, 1993).
- [21] Proceedings of the ECFA workshop on 'e⁺e⁻ Linear Colliders LC 92', ed. R. Settles, Gamisch Partenkirchen, July-August 1992, MPI-PhE/93-14, ECFA 93-154, 1993.
- [22] Proceedings of the I-IV Workshops on Japan Linear Collider', KEK, Japan, 1989, 1990, 1992, 1994, KEK-Reports 90-2, 91-10, 92-1, 94-1.
- [23] A. Sopczak, in Ref. [17], part C.
- [24] W. Kozanecki (convener), in Ref. [17], part B.

- [25] E. Boos, P. Bussey, G. Jikia, D. J. Miller and J. K. Storrow (conveners), in Ref. [17], part C.
- [26] J. F. Gunion and H. E. Haber, report UCD-90-25, 1990 (unpublished); in Proceedings of the Summer Study on High Energy Physics Research Directions for the Decade', Snowmass, Colorado, 1990, ed. E. L. Berger (World Scientific, Singapore, 1991).
- [27] S. Moretti, Phys. Rev. D 50 (1994) 2016.
- [28] D. Bowser-Chao, K. Cheung and S. Thomas, Phys. Lett. B 315 (1993) 399.
- [29] See, e.g.:
 Proceedings of the Workshop Future Physics at HERA', eds. G. Ingelman, A. De Roeck and R. K. Lanner (DESY, Hamburg, 1995-96).
- [30] I. S. Choi, B. H. Cho, B. R. Kim and R. Rodenberg, Phys. Lett. B 200 (1988) 200.
- [31] B. Grzadkowski and W. S. Hou, Phys. Lett. B 210 (1988) 233.
- [32] T. Han and C. Liu, Z. Phys. C 28 (1985) 295.
- [33] G. Abu Leil and S. Moretti, Phys. Rev. D 53 (1996) 178.
- [34] Proceedings of the International Workshop on Linac-Ring Type ep and Gamma-p Colliders', Ankara, Turkey, 9-11 April 1997, to be published in the Turkish Journal of Physics.
- [35] Proceedings of the ECFA Large Hadron Collider Workshop, Aachen, Germany, edited by G. Jarlskog and D. Rein, Geneva, Switzerland, 1990, CERN Report No. 90-10, ECFA Report No. 90-133.
- [36] R. Ruckl, in Ref. [35], Vol. I.
- [37] A. Verdier, in Ref. [35], Vol. III.
- [38] J. Feltesse, in Ref. [35], Vol. I.
- [39] J. L. Diaz-Cruz and O. A. Sampayo, preprint UAB-FT-286/92, May 1992 (unpublished).
- [40] A. Ali, F. Barreiro, J. F. de Troconiz, G. A. Schuler and J. J. van der Bij, in Ref. [35], Vol. II.
- [41] S. Moretti and K. Odagiri, preprint Cavendish-HEP-97/04, August 1997.
- [42] Y. Okada, M. Yamaguchi and T. Yanagida, Prog. Theor. Phys. Lett. 85 (1991) 1;
 J. Ellis, G. Ridol and F. Zwimer, Phys. Lett. B 257 (1991) 83; Phys. Lett. B 262 (1991) 477;
 H. E. Haber and R. Hemping, Phys. Rev. Lett. 66 (1991) 1815;
 R. Barbieri and M. Frigeni, Phys. Lett. B 258 (1991) 395.

- [43] A . Brignole, J . Ellis, G . Ridol and F . Zwimer, Phys. Lett. B 271 (1991) 123;
A . Brignole, Phys. Lett. B 277 (1992) 313;
H E . Haber and M A . Diaz, Phys. Rev. D 45 (1992) 4246.
- [44] V . Barger, K . Cheung, R J N . Phillips and A L . Stange, Phys. Rev. D 46 (1992) 4914.
- [45] G . Ingelman, J . Rathsm an and G . A . Schuler, Comput. Phys. Commun. 101 (1997) 135 (and references therein).
- [46] H1 Collaboration, Z . Phys. C 74 (1997) 191;
ZEUS Collaboration, Z . Phys. C 74 (1997) 207.
- [47] G P . Lepage, Jour. Comp. Phys. 27 (1978) 192.
- [48] T . Stelzer and W F . Long, Comp. Phys. Comm . 81 (1994) 357.

Table C options

- [I] Total cross sections for process (1) at LEP2 LHC energies for twenty-four different sets of structure functions. Errors are as given by VEGAS (the same statistics points were used for the NCALL and ITMX parameters) [47]. As representative values of the MSSM parameters we have used $M_A = 60 \text{ GeV}$ and $\tan \beta = 1.5$.
- [II] Total cross section for process (6) at the LEP2 LHC collider, for a selection of Higgs masses. The structure function set MRS(A) was used. Errors are as given by VEGAS [47]. The following acceptance cuts were implemented: (i) $p_T^+; p_T^b > 20 \text{ GeV}, p_T^{\text{miss}} > 10 \text{ GeV}$ and $R_{+b} > 0.7$.
- [III] Total cross section for process (7) at the LEP2 LHC collider, for a selection of Higgs masses. The structure function set MRS(A) was used. Errors are as given by VEGAS [47]. The following acceptance cuts were implemented: (i) $p_T^+; p_T^b > 20 \text{ GeV}, p_T^{\text{miss}} > 10 \text{ GeV}$ and $R_{+b} > 0.7$.

Figure Captions

- [1] Lowest order Feynman diagrams describing processes (4). The package MadGraph [48] was used to produce the PostScript codes. Graph 1 refers to single-top production and decay whereas graph 2 corresponds to the vector-scalar fusion mechanism.
- [2] The total cross section for process (1) (a,b) and the ratio R between this and that of process (2) (c,d), with $300 \text{ GeV} \leq \sqrt{s_{\text{ep}}} \leq 2 \text{ TeV}$, for $\tan \beta = 1.5$ (a,c) and 30 . (b,d) and for five different values of the pseudoscalar Higgs mass: $M_A = 60 \text{ GeV}$ (continuous lines), $M_A = 100 \text{ GeV}$ (short-dashed lines), $M_A = 140 \text{ GeV}$ (dotted lines), $M_A = 180 \text{ GeV}$ (dot-dashed lines) and $M_A = 220 \text{ GeV}$ (long-dashed lines). The structure function set MRS(A) was used.
- [3] The total cross section for process (6) at the LEP2 LHC CM energy as a function of the pseudoscalar Higgs mass in the range $60 \text{ GeV} \leq M_A \leq 220 \text{ GeV}$, for $\tan \beta = 1.5$ (continuous line) and $\tan \beta = 30$: (dashed line). The structure function set MRS(A) was used.
- [4] The branching ratios of the top quark and charged Higgs boson as a function of the charged (pseudoscalar) Higgs mass in the range $100(60) \text{ GeV} \leq M_H(M_A) \leq 252(240) \text{ GeV}$, for $\tan \beta = 1.5$ and 30 .
- [5] Differential distributions for process (6) at the LEP2 LHC CM energy in the following variables (clockwise): 1. R_b , the azimuthal-pseudorapidity separation of the b -pair; 2. $p_{T, \text{miss}}$, the missing transverse momentum; 3. $p_{T, \ell}$, the transverse momentum of the ℓ -lepton; 4. $p_{T, b}$, the transverse momentum of the b -quark; for $\tan \beta = 1.5$ (a) and 30 . (b) and for three different values of the pseudoscalar Higgs mass: $M_A = 60 \text{ GeV}$ (continuous lines), $M_A = 100 \text{ GeV}$ (dashed lines) and $M_A = 140 \text{ GeV}$ (dotted lines). The normalisation is to unity. The structure function set MRS(A) was used.
- [6] Differential distributions for process (6) at the LEP2 LHC CM energy in the following variables (from top to bottom): 1. M_b , the invariant mass of the b -pair; 2. $|j_b|$, the absolute value of the pseudorapidity of the b -quark; 3. $|j_\ell|$, the absolute value of the pseudorapidity of the ℓ -lepton; for $\tan \beta = 1.5$ (a) and 30 . (b) and for three different values of the pseudoscalar Higgs mass: $M_A = 60 \text{ GeV}$ (continuous lines), $M_A = 100 \text{ GeV}$ (dashed lines) and $M_A = 140 \text{ GeV}$ (dotted lines). The normalisation is to unity. The structure function set MRS(A) was used.
- [7] Differential distributions in the invariant mass of the b -pair, M_b , for processes (7) (e^+b background) and (8) (e^+b background) at the LEP2 LHC CM energy for $M_A = 100 \text{ GeV}$, $\tan \beta = 1.5$ (solid lines) and $\tan \beta = 30$: (dashed lines). The normalisation is to unity. The structure function set MRS(A) was used.

$(e^+ b \rightarrow e b H^+)$	
PDFs	σ_t (fb)
MRS (A)	752.3 2.0
MRS (A')	739.5 1.9
MRS (G)	716.9 1.9
MRS (J)	769.2 2.1
MRS (J')	828.5 2.3
MRS (R1)	701.0 1.9
MRS (R2)	757.8 2.1
MRS (R3)	716.4 1.9
MRS (R4)	766.9 2.0
MRS (105)	673.9 1.8
MRS (110)	718.4 2.0
MRS (115)	712.1 1.9
MRS (120)	772.9 2.1
MRS (125)	778.5 2.1
MRS (130)	791.6 2.2
MRRS (1)	804.4 2.2
MRRS (2)	805.9 2.2
MRRS (3)	803.2 2.2
CTEQ (2M)	782.5 2.1
CTEQ (2M S)	758.3 2.0
CTEQ (2M F)	789.7 2.1
CTEQ (2M L)	843.8 2.3
CTEQ (3M)	832.9 2.3
CTEQ (4M)	815.0 2.3
no acceptance cuts	
LEP2 LHC	

Table I

$\sigma_{\text{tot}}^{\text{signal}} \text{ (fb)}$		
$M_A \text{ (GeV)}$	$\tan \beta = 1.5$	$\tan \beta = 30$
60	194.66 0.87	327.1 1.7
80	140.66 0.62	243.9 1.3
100	76.95 0.40	149.12 0.80
120	24.28 0.14	62.40 0.36
140	2.122 0.010	8.656 0.065
after acceptance cuts		
LEP2 LHC	MRS(A)	

Table II

$\sigma_{\text{tot}}^{e^+b \text{ background}} \text{ (fb)}$		
$M_A \text{ (GeV)}$	$\tan \beta = 1.5$	$\tan \beta = 30$
60	349.1 3.6	341.3 3.7
80	374.6 4.1	358.1 4.3
100	390.9 4.3	384.5 4.6
120	416.6 4.7	413.4 5.0
140	446.5 6.9	439.9 6.3
after acceptance cuts		
LEP2 LHC	MRS(A)	

Table III

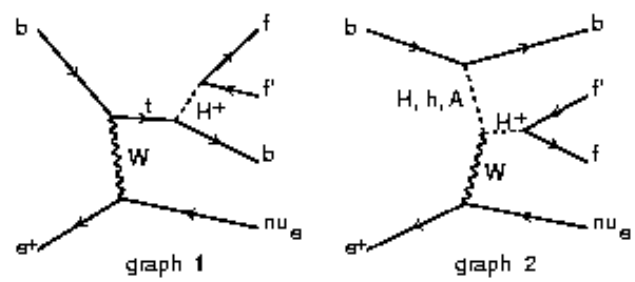


fig. 1

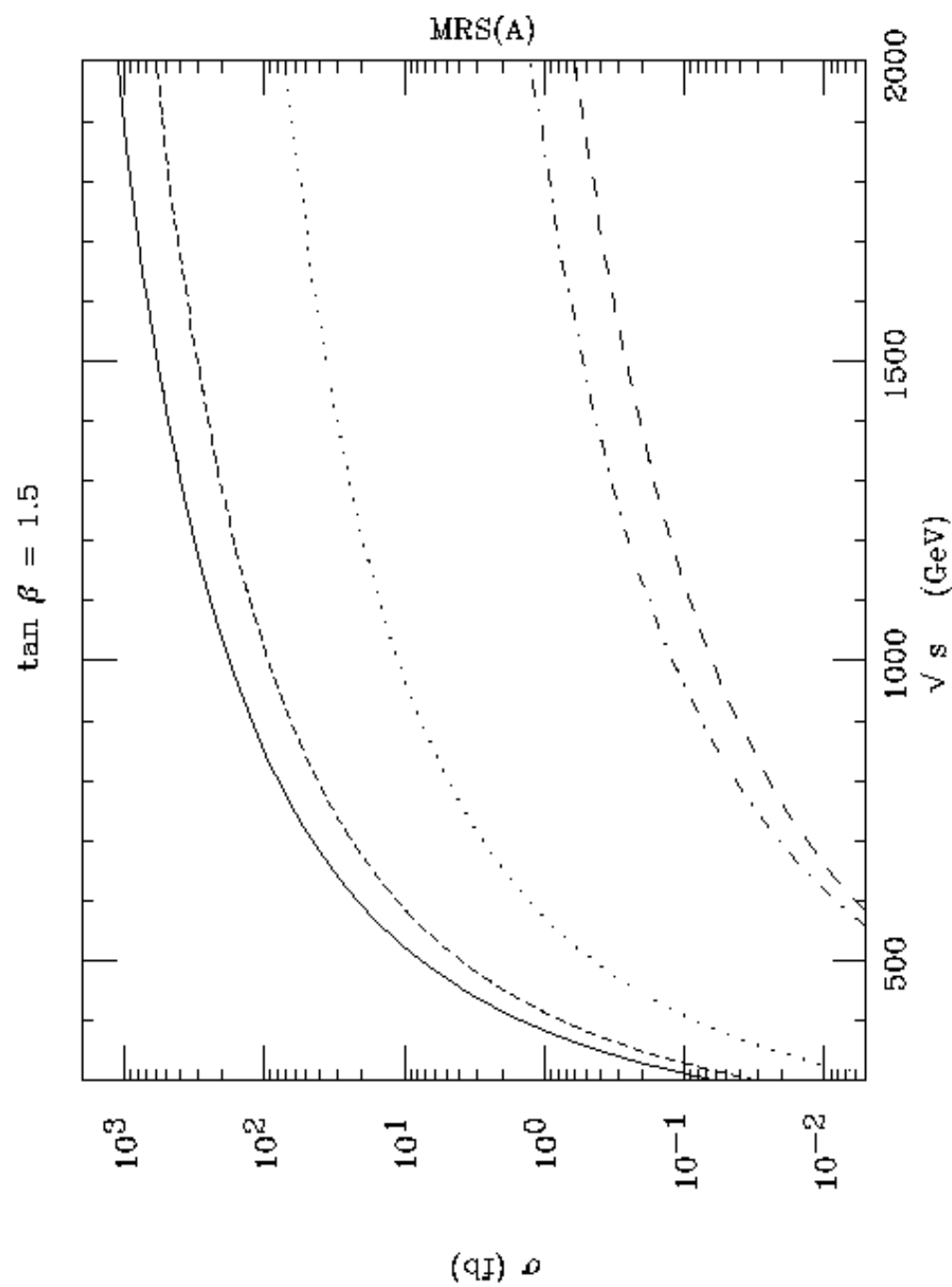


Fig. 2a

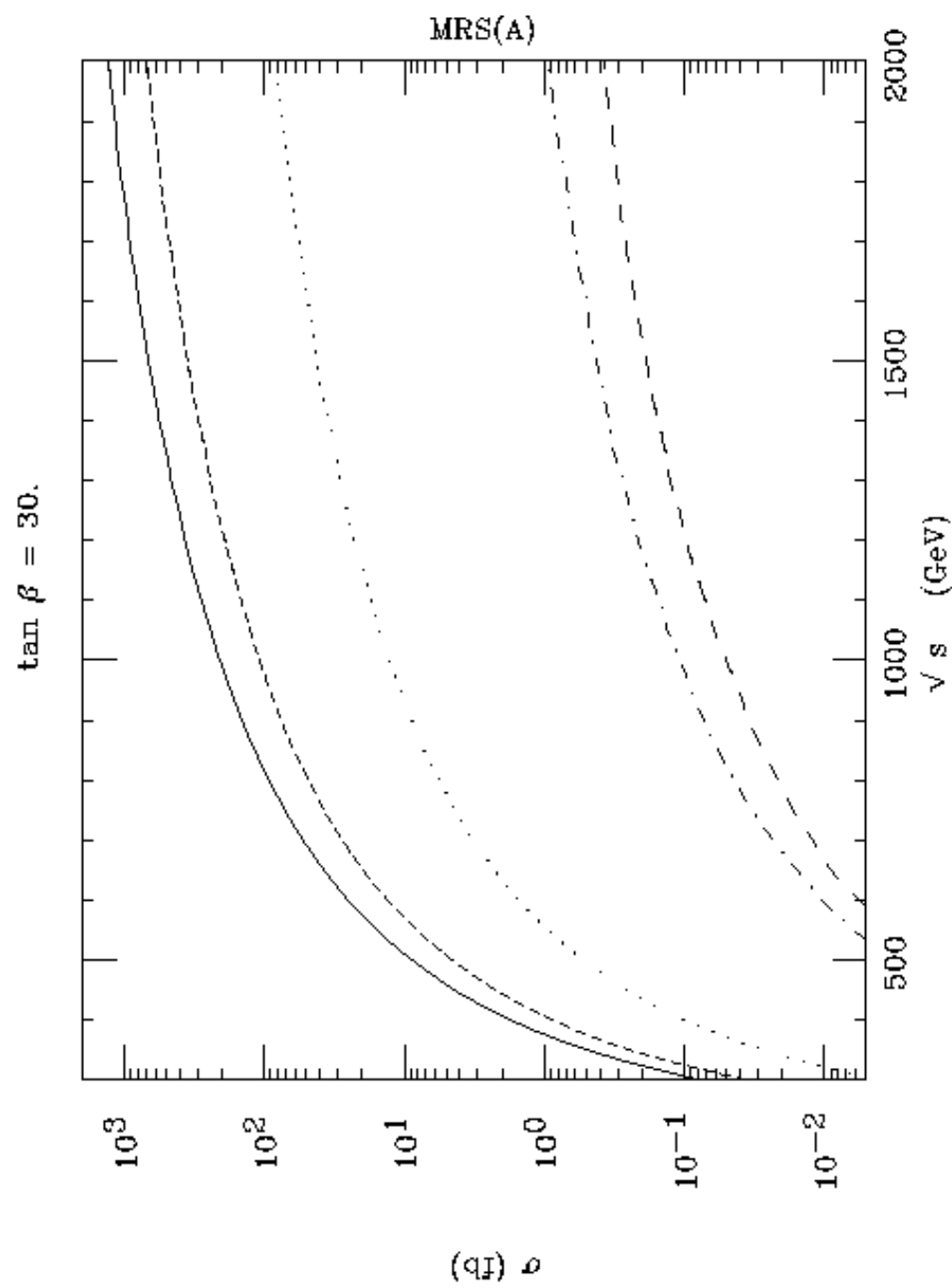


Fig. 2b

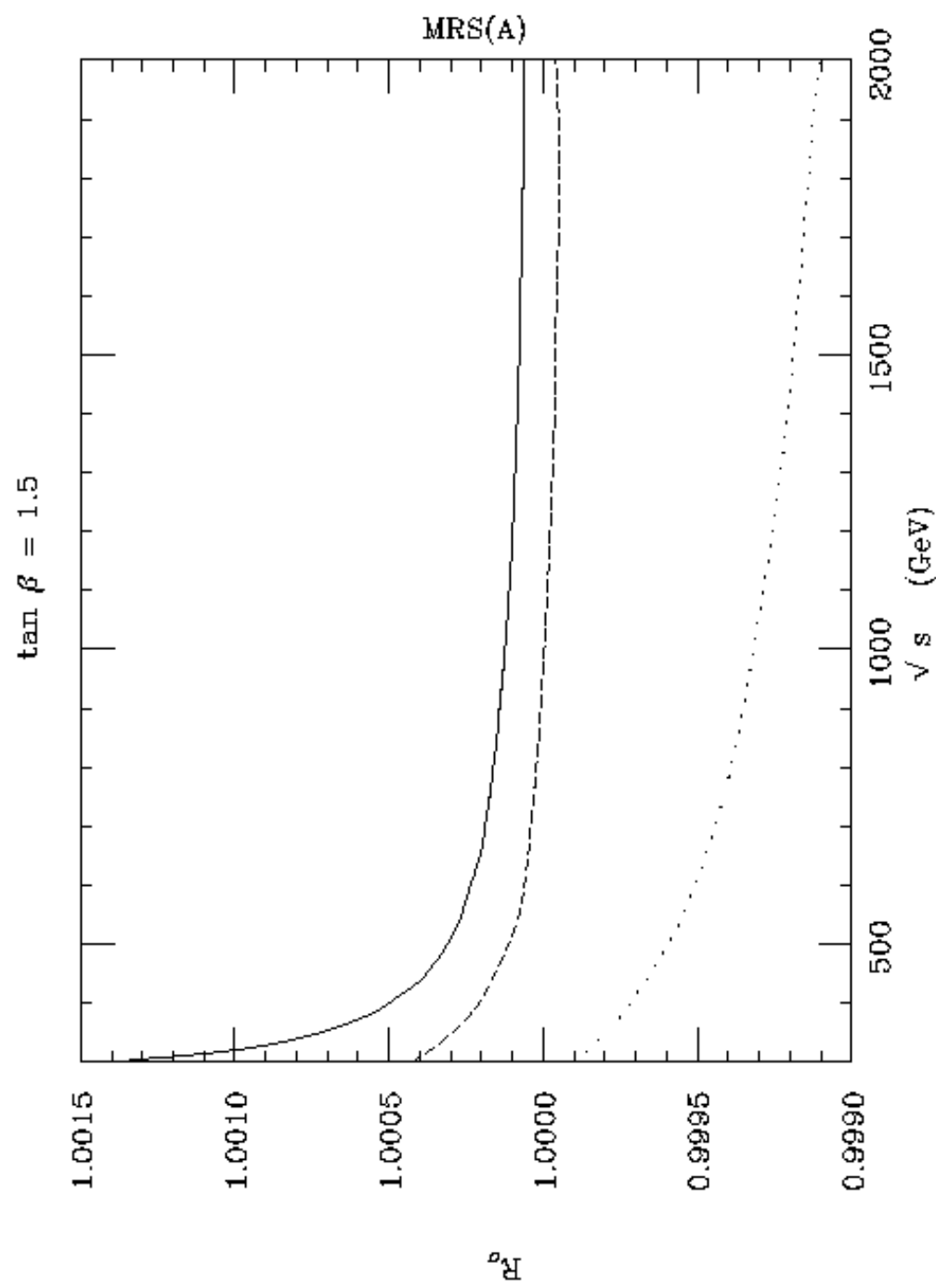


Fig. 2c

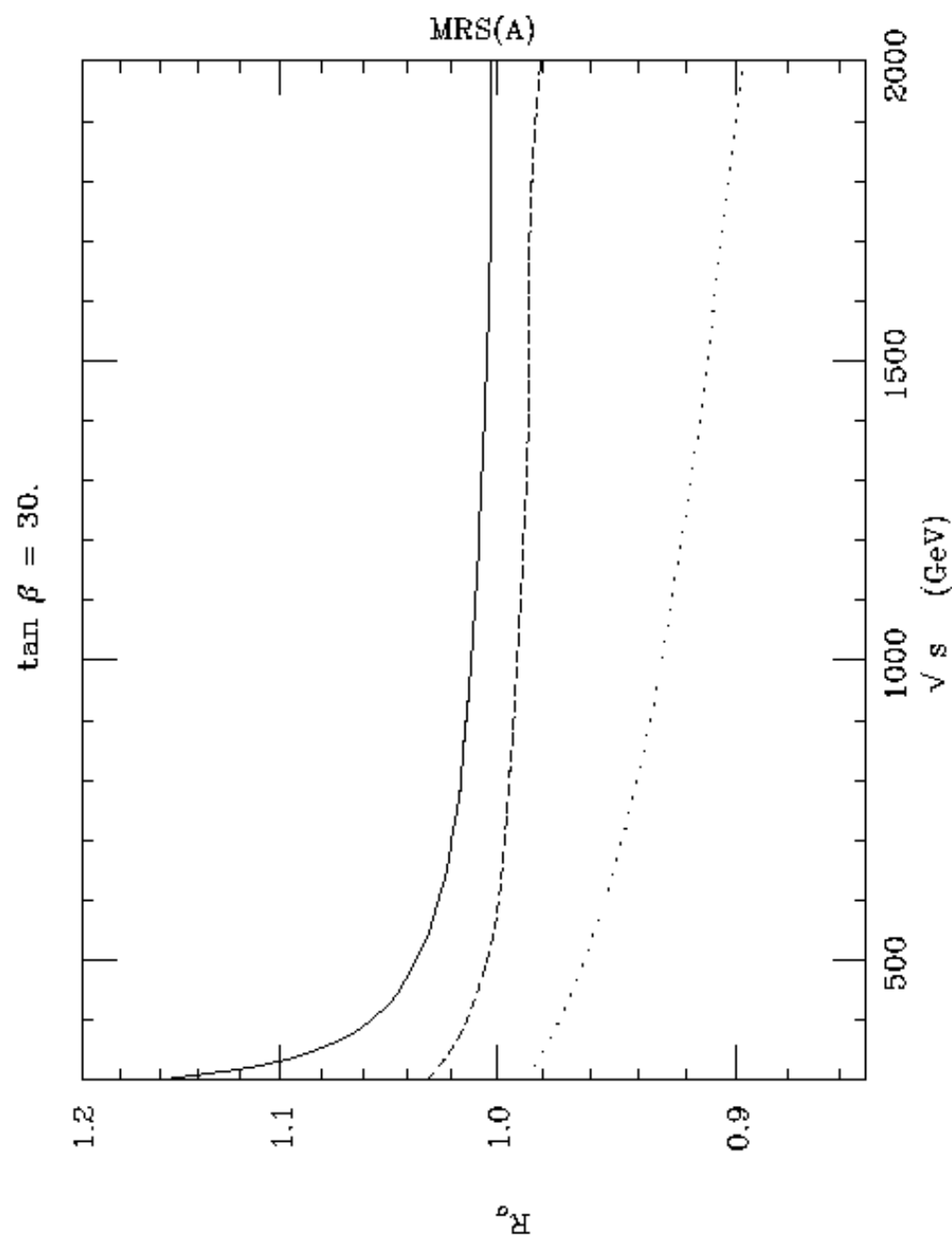


Fig. 2d

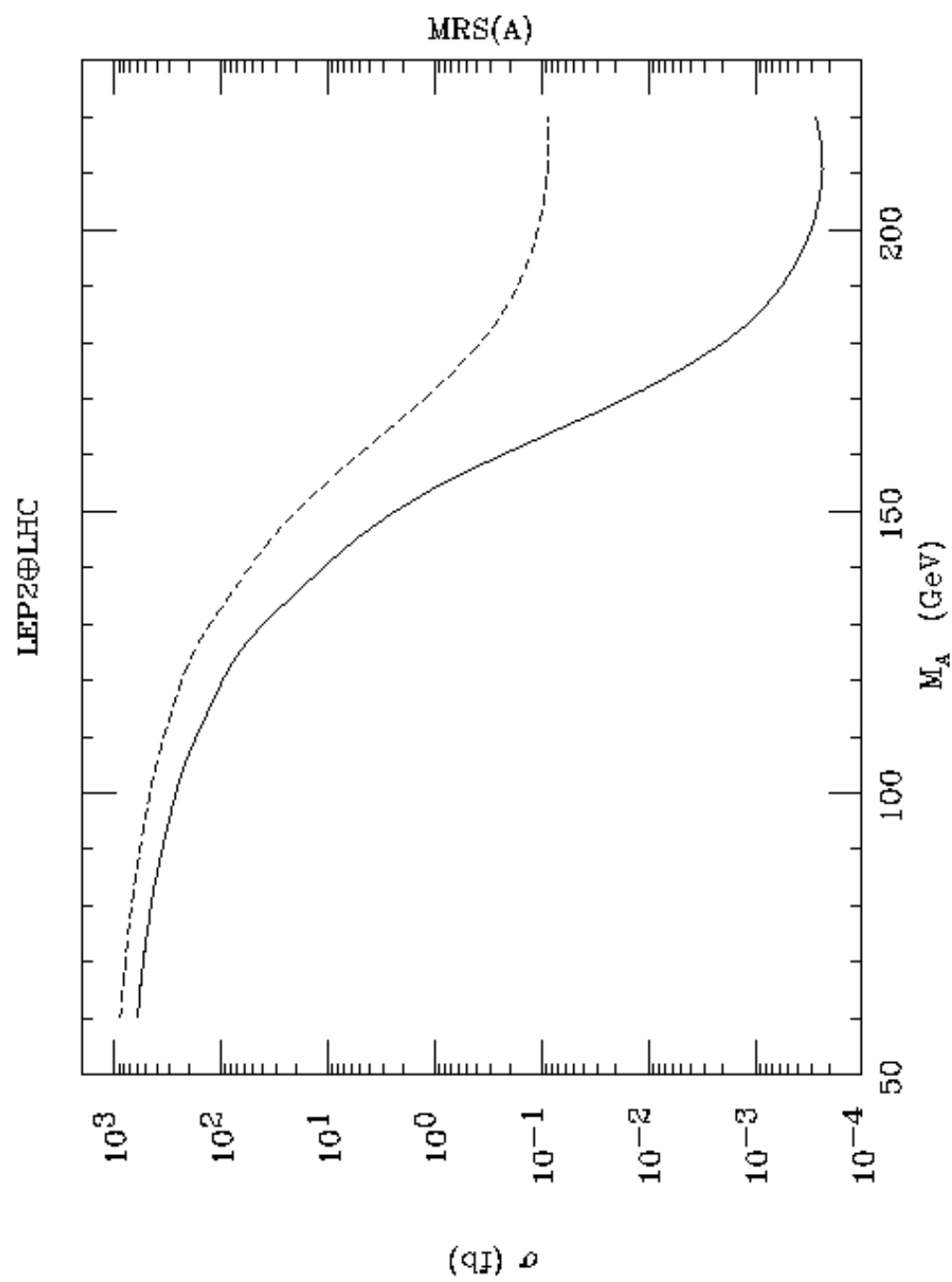


Fig. 3

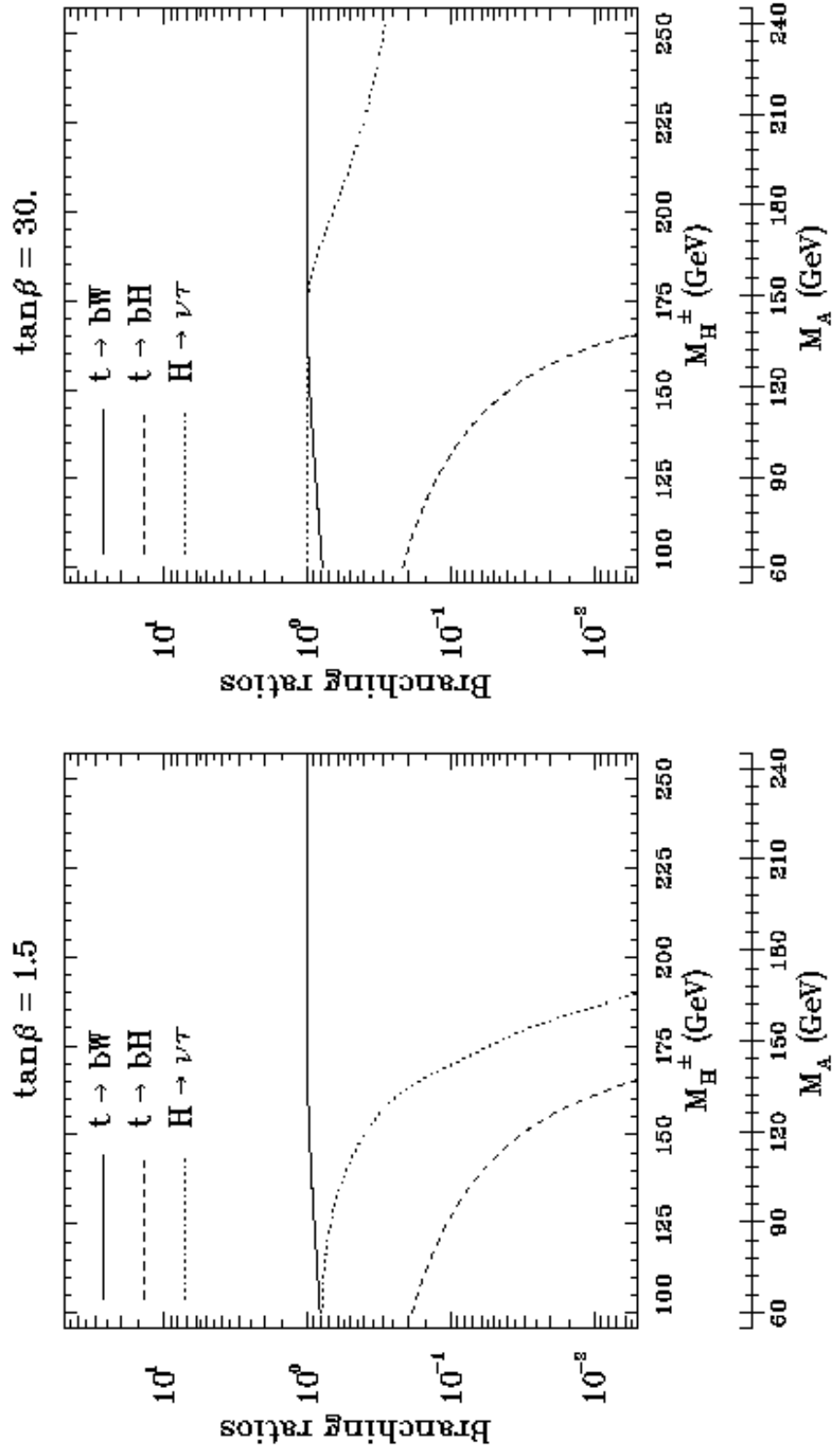


Fig. 4

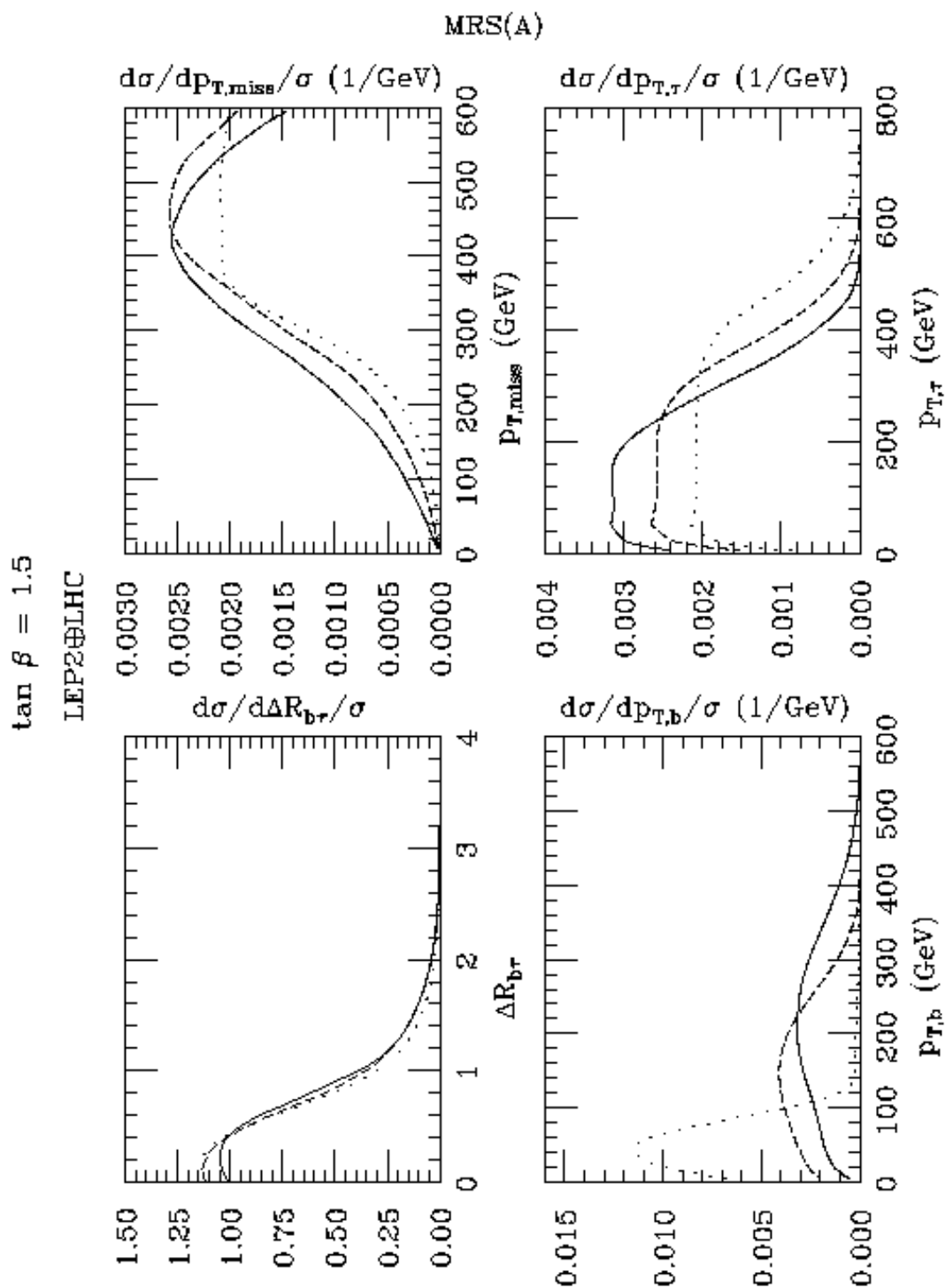
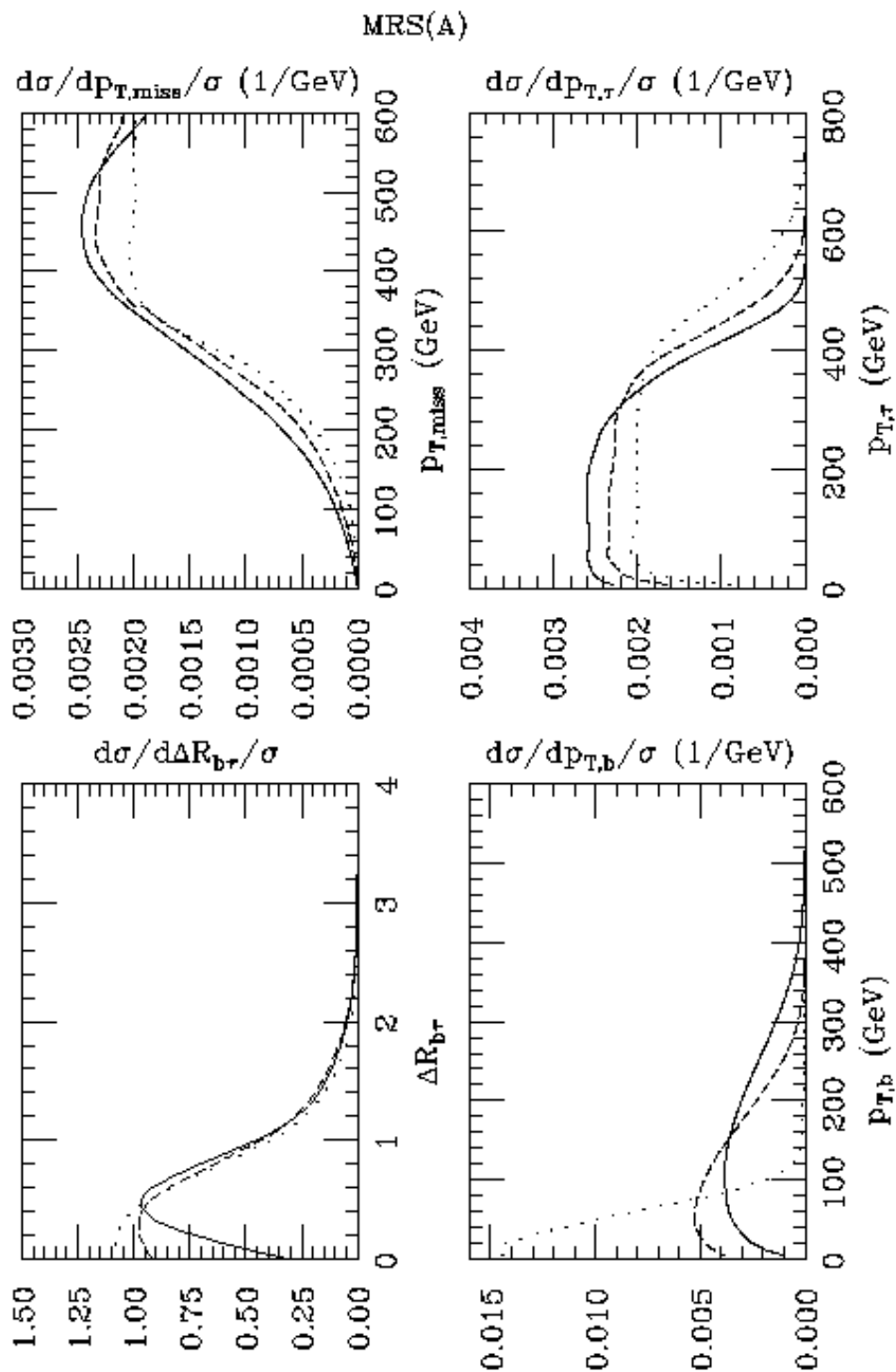


Fig. 5a

$\tan \beta = 30.$

LEP2@LHC



MRS(A)

Fig. 5b

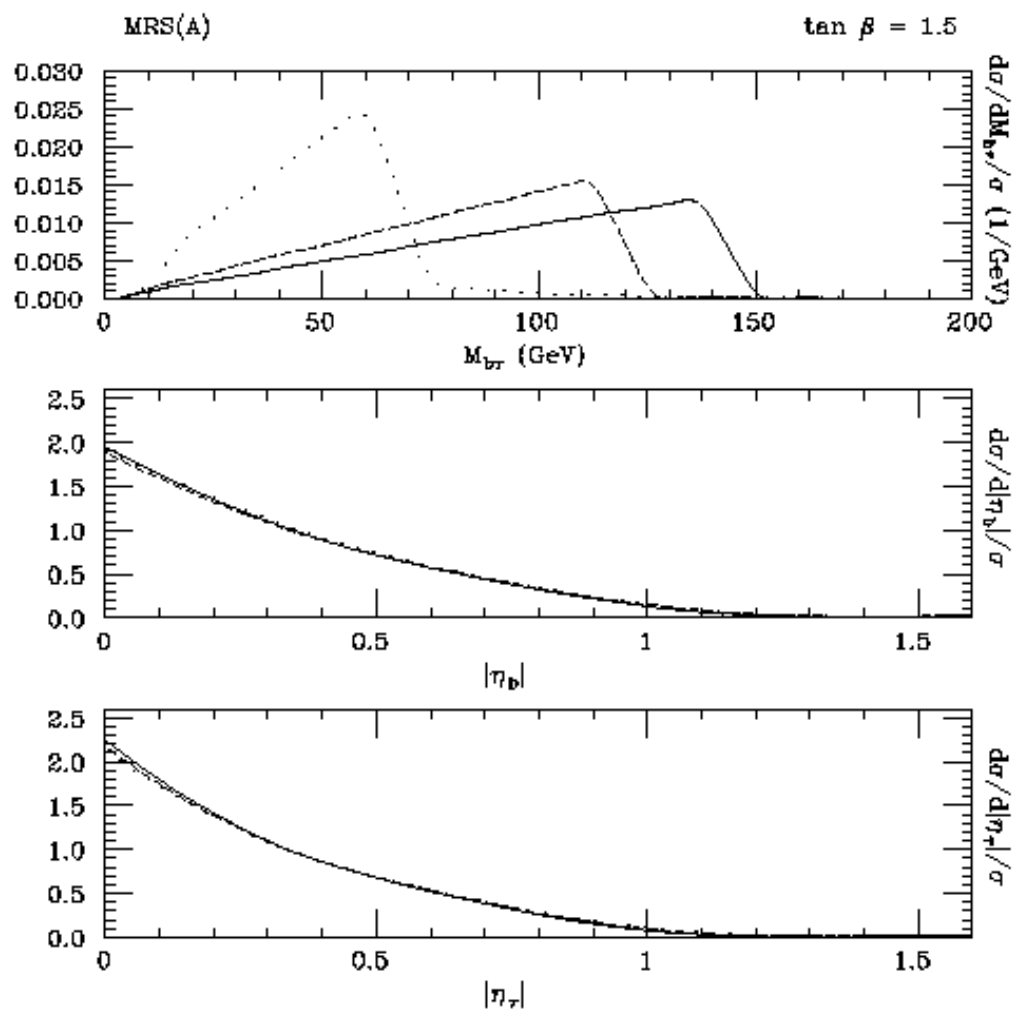


Fig. 6a

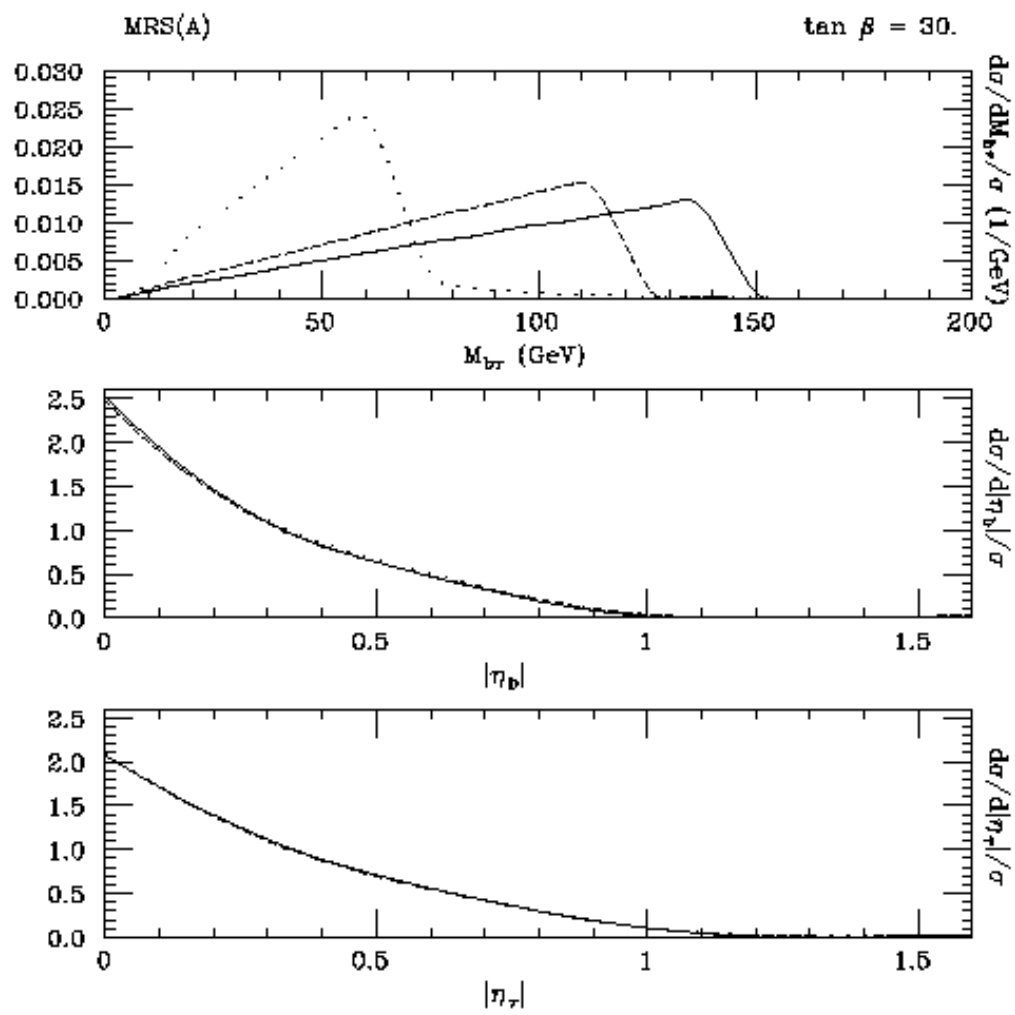


Fig. 6b

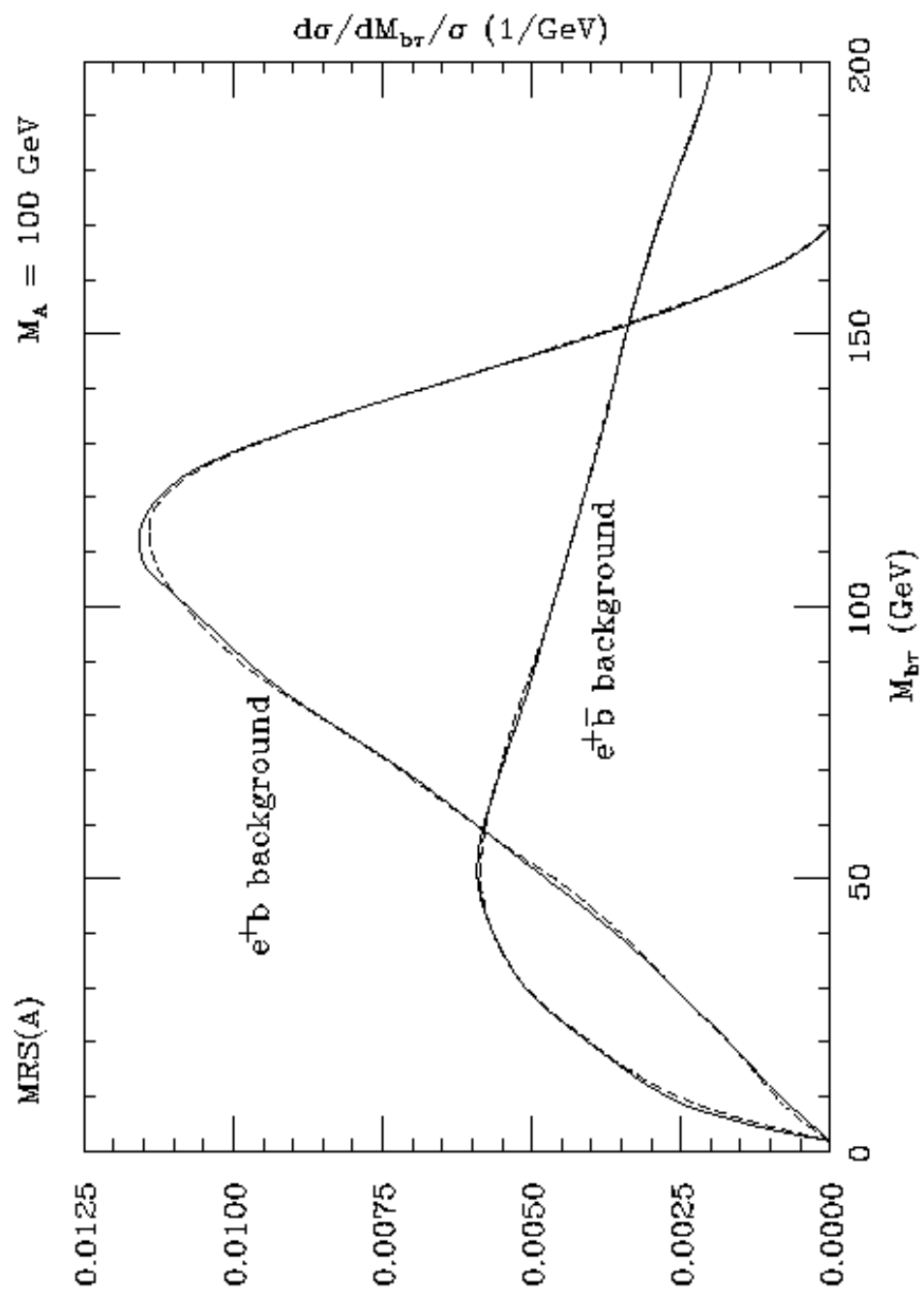


Fig. 7